



Green Combustion Synthesis of CeO₂ and TiO₂ Nanoparticles Doped with Same Oxide Materials of ZrO₂: Investigation of *in vitro* Assay with Antibiotic Resistant Bacterium (ARB) and Anticancer Effect

**A. Mohamed Saleem¹, S. Rajasekar², K. Kaviyarasu^{3,4}, R. Perumalsamy⁵,
A. Ayeshamariam^{5*} and M. Jayachandran⁶**

¹Department of Physics, Jamal Mohamed College, Bharathidasan University, Thiruchirappalli, 620020, India.

²Department of Physics, Syed Ammal Engineering College, Ramanathapuram, 623503, India.

³UNESCO-UNISA Africa Chair in Nanoscience's/Nanotechnology Laboratories, College of Graduate Studies, University of South Africa (UNISA), Muckleneuk Ridge, P.O.Box 392, Pretoria, South Africa.

⁴Nanosciences African Network (NANOAFNET), Materials Research Group (MRG), iThemba LABS-National Research Foundation (NRF), 1 Old Faure Road, 7129, P.O.Box 722, Somerset West, Western Cape, South Africa.

⁵Department of Physics, Khadir Mohideen College, Affiliated to Bharathidasan University, Adirampattinam, Tiruchirappalli, 614701, India.

⁶Department of Physics, Sethu Institute of Technology, Pullor, Kariapatti, 621115, India.

Authors' contributions

This work was carried out in collaboration among all authors. Author AA designed the study and performed the literature survey. Author AMS performed the statistical analysis, wrote the protocol and author KK draft the manuscript. Author RP managed the analyses of the study. Author MJ approved the final manuscript.

Article Information

DOI: 10.9734/EJMP/2019/v30i230171

Editor(s):

(1) Professor, Dr. Patrizia Diana, Section of Medicinal Chemistry and Biology, Department of Molecular and Biomolecular Sciences and Technologies (STEMBIO), University of Palermo, Via Archirafi, 32-90123 Palermo, Italy.

(2) Professor, Marcello Iriti, Professor of Plant Biology and Pathology, Department of Agricultural and Environmental Sciences, Milan State University, Italy.

Reviewers:

(1) Gühergöl Uluçam, Trakya University, Turkey.

(2) V. G. Vidya, University of Kerala, India.

(3) Manohar V. Lokhande, Sathaye College, India.

Complete Peer review History: <http://www.sdiarticle4.com/review-history/52799>

Original Research Article

Received 10 September 2019
Accepted 14 November 2019
Published 19 November 2019

ABSTRACT

This article reports the synthesis, characteristics and biomedical applications of CeO₂-ZrO₂ and TiO₂-ZrO₂ nanoparticles. The nanoparticles are synthesized by Green combustion method. Aloe Vera, dates and pomegranate extracts are used as mediators to avoid toxicity instead of chemical reagents. Hence it is biocompatible, non-toxic and avoiding adverse effect in biomedical applications. The nanoparticles are characterized by XRD to confirm the physical structure. The FTIR, Raman and SEM with EDAX analyses the chemical composition and their morphology. The antibacterial activity of these nanoparticles is assayed by well diffusion method against the bacterial pathogens of *Staphylococcus aureus*, *Shigella flexneri* and *Bacillus sp.* The anticancer effect of the nanoparticles is investigated on A549 cell line by *In Vitro* assay. The conceivable purpose is the hydroxyl radicals which are easily produced by oxidizing more hydroxide ions in alkaline solution. Thus the competence of the development is rationally improved at pH is 9.

Keywords: Green combustion method; antimicrobial; biomedical applications; pathogens; cytotoxicity.

1. INTRODUCTION

Material Science is a research hotspot in the field of nanotechnology and it is about the synthesis, characterization and study of materials in the nanometer region. In this expertise, the intelligent materials are those whose structure which exhibit the new functional and considerably enhanced by biological assets as well as distinct speculate functionalities because of the nanoscale dimensions [1]. In this nanoscale magnitude generally confers the larger surface areas to nanoparticles (NPs) which are compared with macro-sized particles [2]. NPs are known as measured manipulated particle at the atomic level (1-100 nm). They show size related properties significantly from bulk material [3]. In the recent reports, the number of pollutions related with antibiotic resistant bacteria (ARB) has amplified. Microbial infectious viruses are serious health hindrance that has been drawn the communal attention in worldwide as human health threat, which arrays to viable and mutual complications. One functional application of metal nanoparticles as antibacterial agents has been considered as viable tool of biomedical technology where metal NPs are used as bactericidal agents towards human diseases [4]. The intrinsic properties of metal-organic-framework nanocomposites such as Zinc Oxide (ZnO), Titanium Dioxide (TiO₂) and silver (Ag) are mostly characterized by the size, shape elemental composition, crystallinity, morphology and texture matrix. Reducing the size to the nanoscale can modify their chemical, mechanical, electrical, structural morphological and optical properties. These modified features allow the NPs to interact in a unique manner with cell biomolecules and this facilitates the physical

transfer of NPs into the inner cellular structures [5].

Augmented eruptions and poisons of pathogenic strains, bacterial antibiotic resistance, appearance of innovative bacterial transformations, lack of appropriate preparation in underdeveloped countries, and clinic-associated pollutions are wide-ranging health threats to humankind predominantly for products. Defining the efficiency of nanoparticles are an antibacterial mediator involves trial methods (assays) that actions bacteria viability after exposure. Various performances have been established to regulate the antibacterial activity of synthesized nanoparticles, most of them are inconsistent in their peculiar approach. Thus, manifold performances are regularly used in a single analysis to relate the antibacterial consequences. Additionally, Gram +ve and Gram -ve bacteria could respond to antibacterial nanoparticles are inversely and for assays differently [6].

One fundamental application of metal NPs in evaluating antibacterial activity has been considered as the most important tool in biomedical science. Proper incorporation of NPs in to drugs and medicines can basis interaction with disease creating pathogens, there by liberating nanoparticles on the drug superficial, where they meet sarcastic bacteria and cause bacterial inhibition. Infections by bacterial strains, mostly major disease producing pathogens such as *Staphylococcus aureus*, *Shigella flexneri*, *Salmonella sp.* has become more prominent. Therefore, developing NPs as novel antibacterial agents is a new trend and can be applied in various fields such as biosensors, nanomedicine and bio-luminescence technology [7].

2. MATERIALS AND METHODS

2.1 Materials

The source material of TiO₂ was prepared by aqueous sol-gel development grounded on adding of Titanium isopropoxide [Ti(OCH)(CH₃)₂]₄ as alkoxide precursor in the aqueous solution attained by mixing an alcohol with a strong acid. The CeO₂ source material is Ammonium Ce(IV) nitrate [Ce(NO₃)₆H₂O]. The doping material is Zirconium oxide (ZrO₂). Dates and Pomegranate extracts were used as reagents. To study the antibacterial activity, *Staphylococcus aureus*, *Shigella flexneri* and *Bacillus sp.* bacteria were used. For *In Vitro* analysis of anticancer activity, A549 cell line was attained from NCCS, Pune, India. The cells were maintained in DMEM supplemented with 10% FBS, penicillin (100 µg/ml), and streptomycin (100 µg/ml) in a humidified atmosphere of 50 µg/ml CO₂ at 37°C [8].

2.2 Preparation of CeO₂-ZrO₂ and TiO₂-ZrO₂ Nanoparticles

The precursor of CeO₂ and ZrO₂ were taken into the ratio of 90% and 10%. The solutions were prepared for 1 M of CeO₂ (2 gm in 25 ml water) and 0.5 M of ZrO₂ (0.9 gm in 15ml water). Then about 22.5 ml of CeO₂ solution and 1.5 ml of ZrO₂ solution was mixed with dates and Aloe-Vera extracts of each 6 ml drop by drop. The precursor mixed solution was stirred for 30 minutes at 40°C. This mixture was heated through hot plate at 100°C for 15 minutes. Then it was formed as a gel and it was heated by furnace at 250°C for 5 minutes. The sample was mortared to get fine powder. This procedure is illustrated in Fig. 1a. The same procedure was followed to prepare TiO₂-ZrO₂ NPs and illustrated in Fig. 1b. Pomegranate extract (10ml) was used as reagent [9].

2.3 Characterization

The structures and phases of the synthesized NPs were studied by powder X-ray diffraction (XRD) on a X'Pert PRO Diffractometer with CuK α radiation ($\lambda = 1.5406 \text{ \AA}$) and recorded in 2θ values from 10° to 80°. The JCPDS files 89-0555 for TiO₂-ZrO₂ and 81-0792 for CeO₂-ZrO₂ were used to identify the structures and the grain sizes (D), were calculated by Scherrer's equation $D = 0.9\lambda / \beta \cos\theta$, where D is the particle size, λ is the wavelength of X-ray used (0.154 nm), β is the full width at half maximum (FWHM) of the

diffraction peak and θ is the Bragg's angle. Surface areas and volumes of the NPs were calculated. In Fourier transform infra-red (FTIR) analysis the vibration peaks were observed between the 400 and 4000 cm⁻¹ and the functional groups were identified. Raman analysis was carried out in the range 0-5000 cm⁻¹. The morphology of these nanoparticles was observed by scanning electron microscopy (SEM). The mass percentage of the elements presents in TiO₂-ZrO₂ and CeO₂-ZrO₂ NPs were determined by EDX detector (JED-2200 Series standard programs).

2.4 Antibacterial Activity

Bacteria planting are techniques that can be used to estimate bacteria exposure to nanoparticles. This assay is a self-effacing technique to categorize the tentative circumstances twisted a completely antibacterial setting and thus this way to assume the assay governs minimum inhibitory concentrations (MIC) or minimum bactericidal concentrations (MBC). In the contemporary report, Agar plate well diffusion technique was used to investigate the antibacterial effect of the TiO₂-ZrO₂ and CeO₂-ZrO₂ NPs. They were tested for antibacterial properties against the selected bacterial strains namely *Staphylococcus aureus*, *Shigella flexneri* and *Bacillus sp.* which were cultured in nutrient agar medium. A small volume of each bacterial suspension was spread in to the Muller Hinton agar plate. Two wells (4 mm dia.) were made with the help of flamed cork borer on the surface of the agar plate. 25 µL of the test compound and standard (0.1% of streptomycin solution) were placed on walls separately. The plate was incubated at 37±1°C for 24 hrs. After incubation, the diameter of the zone of inhibition (in mm) was measured around the well. Each test was replaced thrice and the mean values were calculated [10].

2.5 Cytotoxicity Measurements

The potential *in vitro* use of NPs as anticancer agents was dependent on cytotoxicity assay in eukaryotic cells. To investigate the anticancer effect of the synthesized NPs, MTT viability assay was used as devised by Mosmann (1983). Cells (1 × 10⁵/well) were placed in 24-well plates and incubated in 37°C with 5% CO₂ order. The synthesized nanoparticles were then supplementary to the cell culture media at various concentration of the sample viz. 7.8, 15.6, 31.2, 62.5, 125, 250, 500 and 1000 µg/ml.

After incubation, the design was removed from the well and rinsed with phosphate buffered saline (pH=7.4), about 100 µl/well of 0.5% 3-(4, 5 di methyl-2-thiazolyl) +2, 5-di phenyl tetra zolium bromide) (MTT) was further and incubated for 4 hrs. The OD value was read at 570 nm with the use of UV-spectrometer. The % of cell viability was considered by the equation; % of cell

viability = (A 570 of treated cells / A 570 of control cells) × 100; the calculated values were plotted on a graph, placing test concentrations (µg/ml) on x-axis and percentage of cell viability values on y-axis. The concentration at 50% of cells inhibition was determined as IC₅₀. Suitable controls both for cells and samples were run each assay to assess the full cell viability [11].

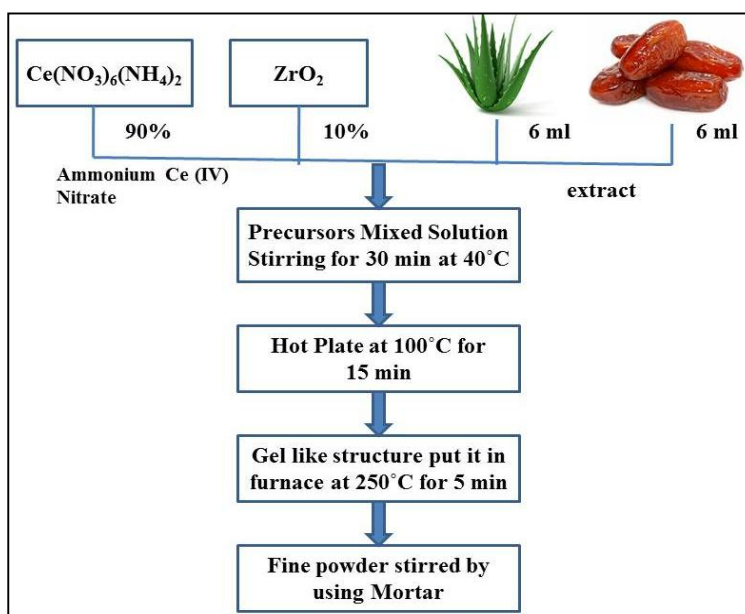


Fig. 1a.

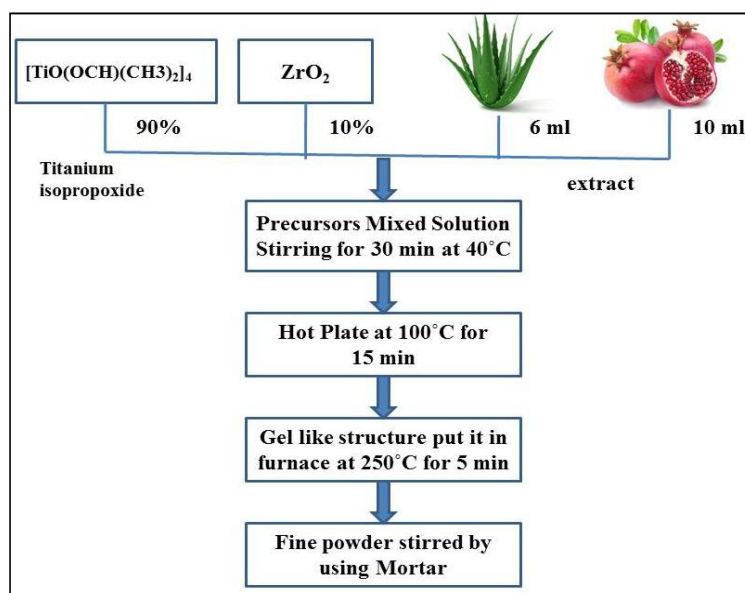


Fig. 1b.

Fig. 1(a-b) Flowcharts for the Synthesis of CeO₂-ZrO₂ and TiO₂- ZrO₂

3. RESULTS AND DISCUSSION

3.1 XRD Analysis

The structural identification of $\text{CeO}_2\text{-ZrO}_2$ and $\text{TiO}_2\text{-ZrO}_2$ nanoparticles was done by X-ray diffraction as shown in Fig. 2. The diffraction peaks of $\text{CeO}_2\text{-ZrO}_2$ nanoparticles (111), (200), (220), (311), (222), (400), (331) and (420) were obtained. The peaks are in prompt agreement with the typical diffraction spectrum (JCPDS file 81-0792). It was clearly indicated that the fine crystalline and single phase of $\text{CeO}_2\text{-ZrO}_2$, could be indexed to the cubic structure. The diffraction peaks of $\text{TiO}_2\text{-ZrO}_2$ nanoparticles (110), (101), (111), (211), (220), (002) and (301) matched with JCPDS file 89-0555, the diffraction peaks are indexed to the tetragonal planes. The average crystallite sizes, volumes, lattice parameters and surface areas of these nanoparticles are shown in Table 1.

3.2 FTIR and Raman Analysis

Fig. 3 shows the FTIR spectra of the $\text{CeO}_2\text{-ZrO}_2$ and $\text{TiO}_2\text{-ZrO}_2$ nanoparticles in the wavelength range of 4000 cm^{-1} – 400 cm^{-1} . The alteration of dipole moment of bonds takes place with vibration effects in IR region. In the present study, the nanoparticles contain of Ce-O, Ti-O and Zr-O bonds which have sensible dipole moment. Oxide materials which have more attention than one oxygen atom bound to a single metal atom frequently engage in the region of 1050 cm^{-1} - 870 cm^{-1} [12]. Due to the

nanosized effect, the Ce-O, Ti-O and Zr-O stretching vibrations may be found in the region of 980 cm^{-1} - 300 cm^{-1} . In our study, the spectra of both illustrations exhibited similar peak which was observed at 1383 cm^{-1} belonged to CH_3 group of FTIR band spectrum. The other peaks observed for $\text{CeO}_2\text{-ZrO}_2$ nanoparticles are 486, 742, 1625 and 2932 cm^{-1} and for $\text{TiO}_2\text{-ZrO}_2$ nanoparticles are 665, 1587 and 2894 cm^{-1} . The band at $\sim 1625\text{ cm}^{-1}$ was consigned to the hydroxyl deformation mode of aquatic molecules and specified the presence of physisorbed water on the binary oxides [13,14]. The peak at $\sim 2900\text{ cm}^{-1}$ is primarily due to the stretching vibration of C- CH_3 . Hence, the study revealed that both $\text{CeO}_2\text{-ZrO}_2$ and $\text{TiO}_2\text{-ZrO}_2$ NPs have a high concentration of CH_3 groups. It is known that when the excitation wavelength is close to an electronic transition, Raman scattering changes from normal to resonant, which can result in sufficient increasing of signal intensities (Fig. 4). Resonance process can enhance one type of vibration modes, while the others remain unaffected [15]. In the present study, the peaks were observed at 1531 cm^{-1} and 1581 cm^{-1} for $\text{CeO}_2\text{-ZrO}_2$ and $\text{TiO}_2\text{-ZrO}_2$ nanoparticles respectively.

3.3 SEM and EDX Analysis

The morphologies of $\text{CeO}_2\text{-ZrO}_2$ and $\text{TiO}_2\text{-ZrO}_2$ nanoparticles were studied by SEM analysis. From Figs. 5(a) and 6(a) it is recognized that both samples are appeared in spherical form.

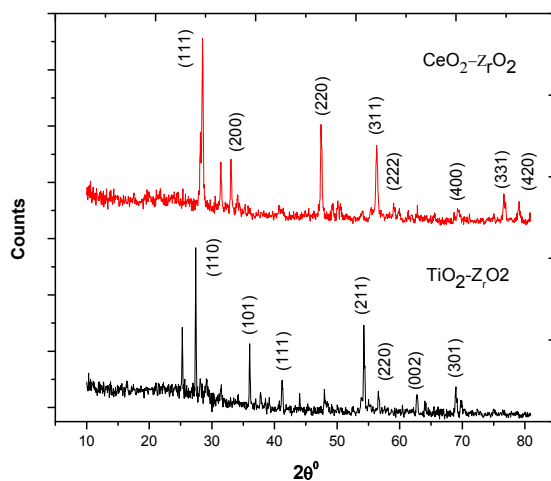


Fig. 2. XRD pattern of $\text{CeO}_2\text{-ZrO}_2$ and $\text{TiO}_2\text{-ZrO}_2$

Table 1. XRD analysis of CeO₂-ZrO₂ and TiO₂-ZrO₂ $\lambda = 1.54056 \text{ \AA}$

Sample	Grain size D (nm)	Strain ξ	Dislocation density ($1/D^2$) (Lines/m ²)	Lattice parameter		Surface area (m ² /gm)	Texture coefficient	Volume V m ³
				a (Å)	c (Å)			
CeO ₂ -ZrO ₂ (Cubic)	43.5237	0.000758	0.0003948	5.416	----	21.572	0.87807	158.9045
TiO ₂ -ZrO ₂ (Tetragonal)	57.8921	0.001965	0.0006805	4.5995	2.9668 Å	28.993	0.80871	62.766

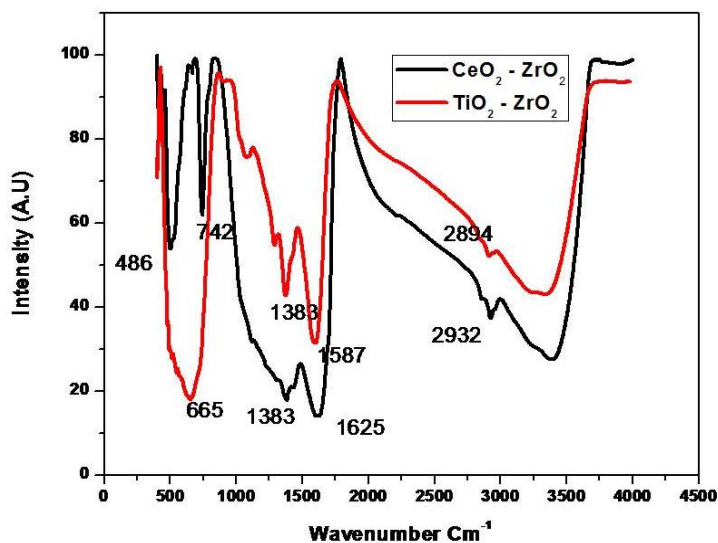


Fig. 3. FTIR analysis of $\text{CeO}_2\text{-ZrO}_2$ and $\text{TiO}_2\text{-ZrO}_2$

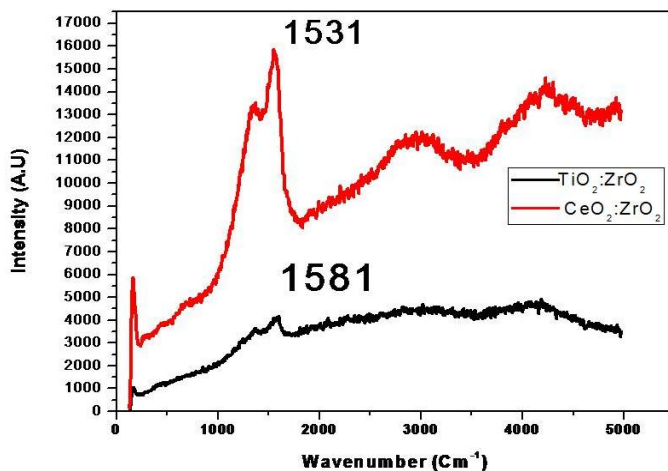


Fig. 4. Laser Raman spectrum of $\text{CeO}_2\text{-ZrO}_2$ and $\text{TiO}_2\text{-ZrO}_2$

Table 2. SEM and EDAX analysis of $\text{CeO}_2\text{-ZrO}_2$

Element	(KeV)	Mass%	Error%	At%
O-K	0.525	18.94	1.70	63.10
Zr-L	2.042	29.74	7.73	17.38
Ce-K	4.837	51.31	33.30	19.52
Total		100.00		100.00

Table 3. SEM and EDAX analysis of $\text{TiO}_2\text{-ZrO}_2$

Element	(KeV)	Mass%	Error%	At%
Ti-K	4.508	95.00	24.64	94.07
O-L	1.023	2.89	1.036	4.81
Zr-K	1.021	2.11	19.12	1.12
Total		100.00		100.00

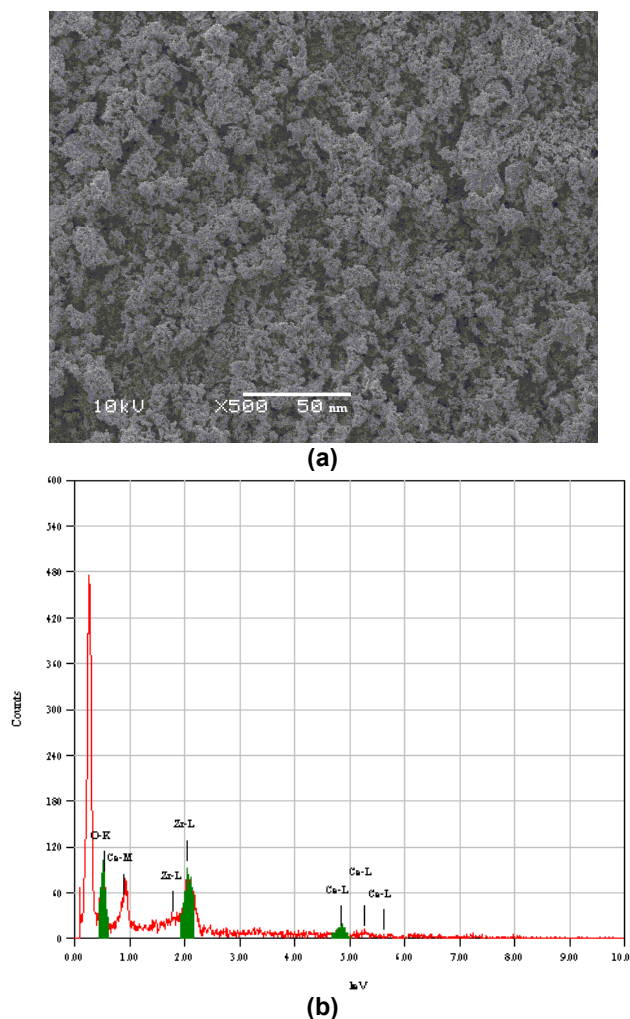


Fig. 5(a-b). SEM and EDAX analysis of ZrO_2 doped with CeO_2

The TiO_2 - ZrO_2 nanoparticles are very smaller in morphology when compared with CeO_2 - ZrO_2 nanoparticles. The elemental dispersive analysis (EDX) completes the chemical profile of the CeO_2 - ZrO_2 nanoparticles which has 51.31% of cerium, 29.74% of zirconium and 18.94% of oxygen. Also, it has shown high atomic percentage as 19.52% of cerium, 17.38% of zirconium and 63.10% of oxygen Fig. 5(b). Concerning TiO_2 - ZrO_2 nanoparticles, the chemical profile was noted as 97.89% of titanium and 2.11% of zirconium. In addition, it was observed that there was a high atomic percentage as 98.88% of titanium and 1.12% of zirconium Fig. 6(b).

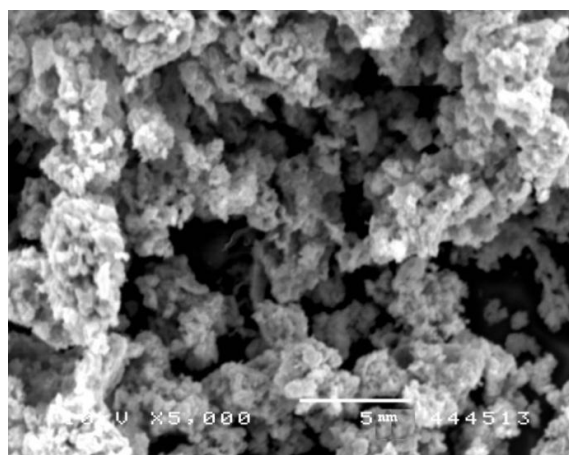
3.4 Antibacterial Activity

The bacterial film is usually packed with the various proteins of CeO_2 - ZrO_2 nanoparticles

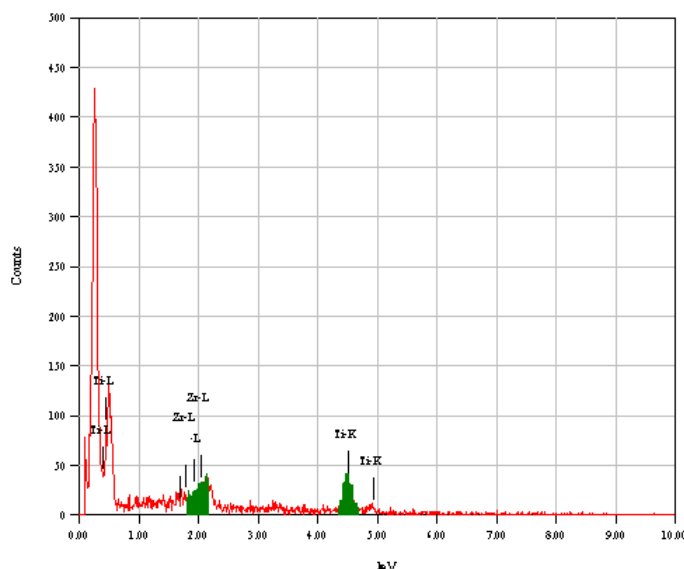
have the competence to get shortest attachment with the cell membrane and can interrelate with the proteins existing in the cell membrane and DNA. This interaction may lead to tear down the respiratory chain following cell death [16,17-20]. The antibacterial activity of CeO_2 - ZrO_2 and TiO_2 - ZrO_2 nanoparticles was analyzed in vitro using well diffusion method. The bactericidal effect was confirmed in contradiction of gram negative bacteria *S. flexneri* and gram positive pathogens like *S. aureus* and *Bacillus sp.* The antibacterial activity of CeO_2 - ZrO_2 and TiO_2 - ZrO_2 nanoparticles was given in Tables 4 and 5 respectively. Regarding CeO_2 - ZrO_2 nanoparticles, the zone of inhibition was bigger against *S. aureus* (23 mm) rather than against other pathogens. But when compared to standard (34 mm), the inhibition zone is much lesser Fig. 7(a). In case of *S. flexneri*, it was 26 mm, only a bit lesser than standard (29 mm) Fig.

7(b). But in the case of *Bacillus sp.*, the inhibition zone (34 mm) is greater than the inhibition zone of standard (32 mm) Fig. 7(c). Similarly, for TiO₂-ZrO₂ nanoparticles, *S. aureus* showed better inhibition zone (25 mm) than other pathogens but not when compared to standard (34 mm) Fig. 7(d). Both *S. flexneri* (31 mm) and *Bacillus sp.* (39 mm) displayed bigger inhibition zone than standard (29 and 32 mm respectively) Fig. 7(e-f) this was clearly illustrated in the graph Fig. 8. In previous studies reported that; TiO₂ nanotubes own antimicrobial accomplishment and the device involves a prompt and reversible substantial first phase, and a cellular second phase [21,22-27]. Another study compared the antibacterial activity of Ti substrate with Ti coated

with EG, PEG 400, PEG 600 and PEG 1000 against *E. coli*. Among these, Ti substrate showed little activity [28,29]. This reveals that Ti substrate has not much antibacterial activity. Studies about the bactericidal activity of ZrO₂ nanoparticles disclosed that they exhibit greater activity against *S. aureus* and *B. subtilis* [30,31, 32]. In the case of CeO₂ nanoparticles, studies suggested that they have competent activity against gram negative bacteria like *E. coli* than gram positive bacteria *S. aureus* [33]. These studies reveal that the CeO₂ and TiO₂ nanoparticles have activity towards bacteria but when doped with ZrO₂ nanoparticles, the activity got boost up which leads to inhibition zone even greater than standard antibiotic.



(a)



(b)

Fig. 6(a-b). SEM and EDAX spectrum of TiO₂-ZrO₂

Table 4. Antimicrobial activity of the CeO₂-ZrO₂ treated against bacterial pathogens

Test organisms	Zone of inhibition in millimeter (in diameter)	
	CeO ₂ -ZrO ₂	Standard Streptomycin 30µg
<i>Staphylococcus aureus</i>	23	34
<i>Shigella flexneri</i>	26	29
<i>Bacillus sp</i>	34	32

Solvent used: DMSO (Dimethyl Sulphoxide)
Standard used: Streptomycin 30 µg

Table 5. Antimicrobial activity of the TiO₂-ZrO₂ treated against bacterial pathogens

Test organisms	Zone of inhibition in millimeter (in diameter)	
	TiO ₂ -ZrO ₂	Standard Streptomycin 30µg
<i>Staphylococcus aureus</i>	25	34
<i>Shigella flexneri</i>	31	29
<i>Bacillus sp</i>	39	32

Solvent used: DMSO (Dimethyl Sulphoxide)
Standard used: Streptomycin 30 µg

Table 6. Anticancer effect of CeO₂-ZrO₂ on A549 cell line

S. No.	Concentration (µg/ml)	Dilutions	Absorbance (O.D)	Cell viability (%)
1	1000	Neat	0.071	14.31
2	500	1:1	0.161	32.45
3	250	1:2	0.214	43.14
4	125	1:4	0.261	52.62
5	62.5	1:8	0.305	61.49
6	31.2	1:16	0.361	72.78
7	15.6	1:32	0.401	80.84
8	7.8	1:64	0.439	88.50
9	Cell control	-	0.496	100

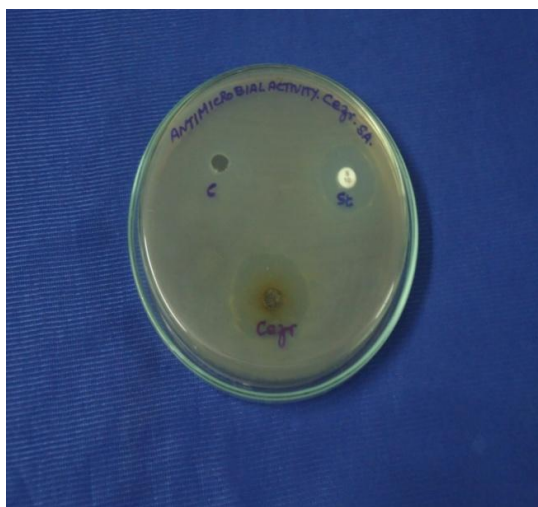
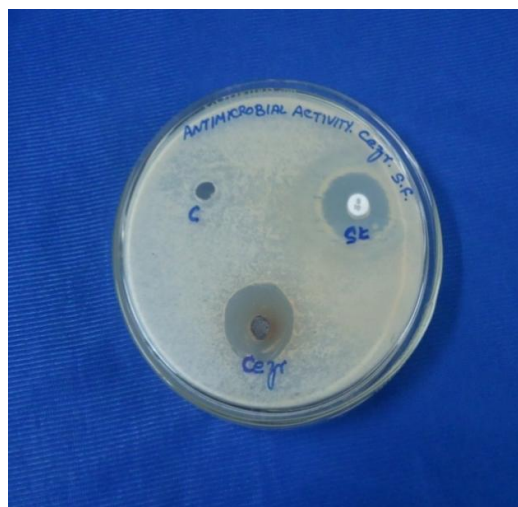
**Fig. 7a. Antimicrobial activity of compounds treated against *Staphylococcus aureus* using by well diffusion method of CeO₂-ZrO₂****Fig. 7b. Antimicrobial activity of compounds treated against *Shigella flexneri* using by well diffusion method of CeO₂-ZrO₂**



Fig. 7c. Antimicrobial activity of compounds treated against *Bacillus sp* using by well diffusion method of CeO_2-ZrO_2

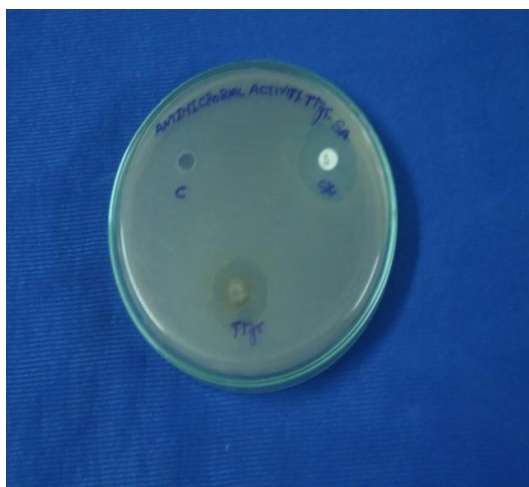


Fig. 7d. Antimicrobial activity of compounds treated against *Staphylococcus aureus* using by well diffusion method of TiO_2-ZrO_2



Fig. 7e. Antimicrobial activity of compounds treated against *Shigella flexneri* using by well diffusion method of TiO_2-ZrO_2



Fig. 7f. Antimicrobial activity of compounds treated against *Bacillus sp* using by well diffusion method of TiO_2-ZrO_2

Table 7. Anticancer effect TiO_2-ZrO_2 on A549 cell line

S. No.	Concentration ($\mu\text{g/ml}$)	Dilutions	Absorbance (O.D)	Cell Viability (%)
1	1000	Neat	0.062	12.50
2	500	1:1	0.107	21.57
3	250	1:2	0.165	33.26
4	125	1:4	0.204	41.12
5	62.5	1:8	0.247	49.79
6	31.2	1:16	0.316	63.70
7	15.6	1:32	0.375	75.60
8	7.8	1:64	0.413	83.26
9	Cell control	-	0.496	100

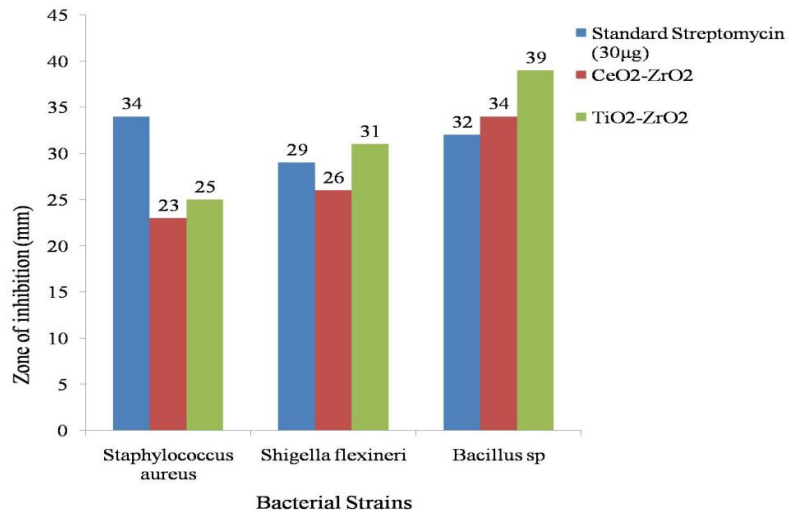


Fig. 8. Comparative bar chart of CeO₂-ZrO₂ and TiO₂-ZrO₂ with standard streptomycin (30 µg)

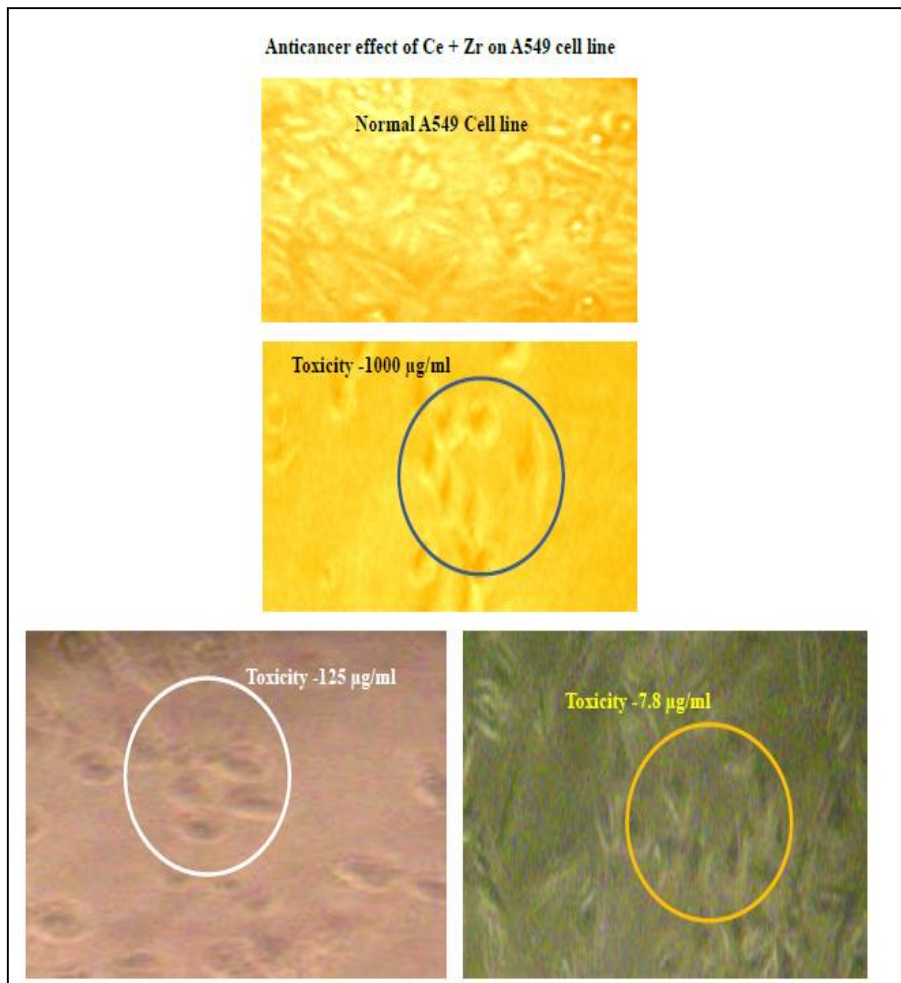


Fig. 9a.

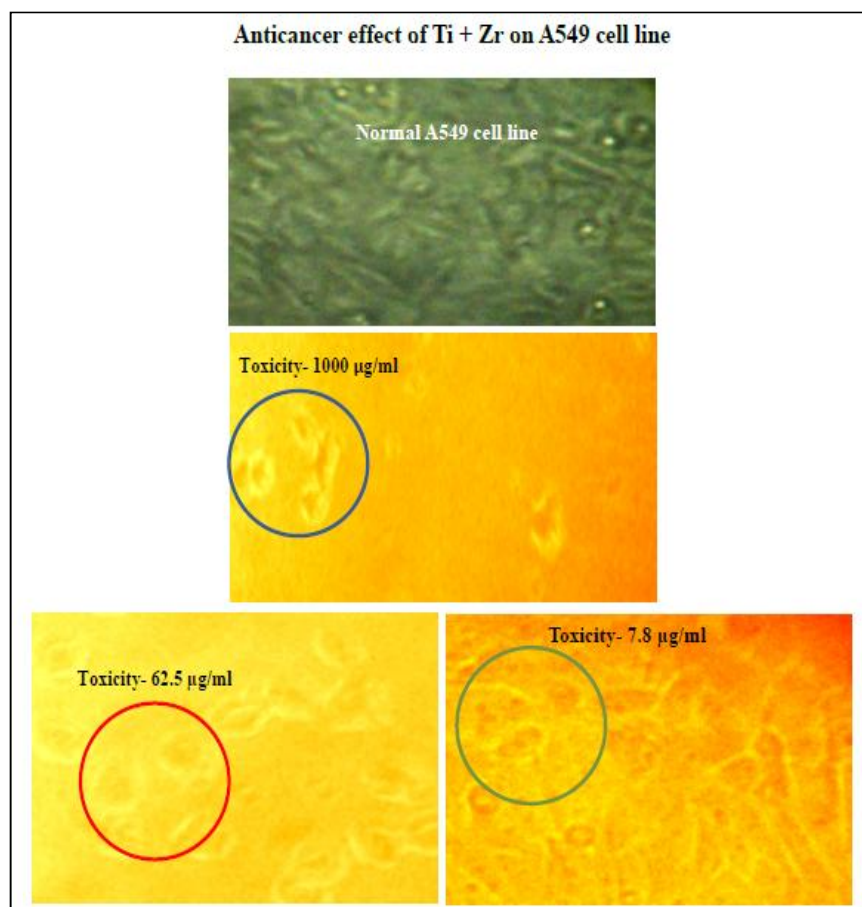


Fig. 9b.

Fig. 9 (a-b). Cytotoxicity result analysis of $\text{CeO}_2\text{-ZrO}_2$ and $\text{TiO}_2\text{-ZrO}_2$

3.5 Cytotoxicity Behavior

The significant candidate of anticancer drug is the ability to induce tumor cell apoptosis [34,35-37]. The basic cytotoxic assay to assess anticancer activity is MTT assay. In the present study, various concentrations of $\text{CeO}_2\text{-ZrO}_2$ and $\text{TiO}_2\text{-ZrO}_2$ nanoparticles were treated against A549 cell line. The percentage of cell viability was gradually decreased against increasing concentration of nanoparticles Table 7. Both $\text{CeO}_2\text{-ZrO}_2$ and $\text{TiO}_2\text{-ZrO}_2$ nanoparticles showed obvious results against A549 cell line. The nanoparticles showed good activity against A549 cells even at lower concentration like 7.8 $\mu\text{g/ml}$. When comparing the cytotoxic property of two nanoparticles, the $\text{TiO}_2\text{-ZrO}_2$ nanoparticles showed better activity rather than $\text{CeO}_2\text{-ZrO}_2$ nanoparticles. The IC_{50} values of $\text{CeO}_2\text{-ZrO}_2$ and $\text{TiO}_2\text{-ZrO}_2$ nanoparticles are 52.62 and 49.79 respectively. This indicated that

nanoparticles showed intense activity against A549 cell line in Fig. 9a. A recent study [38] showed the anticancer activity of TiO_2 nanoparticles against A549 cells, which confirmed that cell viability got decreased only after 72 hrs of treatment. But in the present study, the results illustrated that $\text{TiO}_2\text{-ZrO}_2$ nanoparticles impart cytotoxic effect towards the A549 cell line with 24 hrs treatment. Another study about the cytotoxic effect of CeO_2 nanoparticles on different cell lines reported that these nanoparticles were careful drive cancer cells screening growth and thought-provoking effect in normal cells [39]. Hence, it is evident that the both TiO_2 and CeO_2 nanoparticles do not possess efficient cytotoxic activity towards A549 cell line. But the doping of ZrO_2 nanoparticles with those enhances the cytotoxic ability of both CeO_2 and TiO_2 nanoparticles. For the preliminary classification of the cytotoxicity encouraged by the nanoparticles of A549 cancer

cell, the deviations in cell morphology induced by the treatment of $\text{CeO}_2\text{-ZrO}_2$ and $\text{TiO}_2\text{-ZrO}_2$ nanoparticles was first surveyed under a phase contrast microscope. The cancer cell lines showed cell decline, membrane blebbing and loss of cell adhesion which were tempted by the nanoparticles in Fig. 9b. These cellular variations are the characteristics of the apoptotic induction of cell death. This demonstrated that the nanoparticles of our study use the apoptotic

pathway to kill the cancer cells but not the necrosis pathway as shown in Fig. 9. This further illustrated that the nanoparticles of our study are good candidates, which possess cytotoxic ability against A549 cell line. In addition, the previous studies also showed that both CeO_2 and TiO_2 nanoparticles are non-reactive towards normal cell line. This indicated that $\text{CeO}_2\text{-ZrO}_2$ and $\text{TiO}_2\text{-ZrO}_2$ nanoparticles can be further tested for *in vivo* trials.

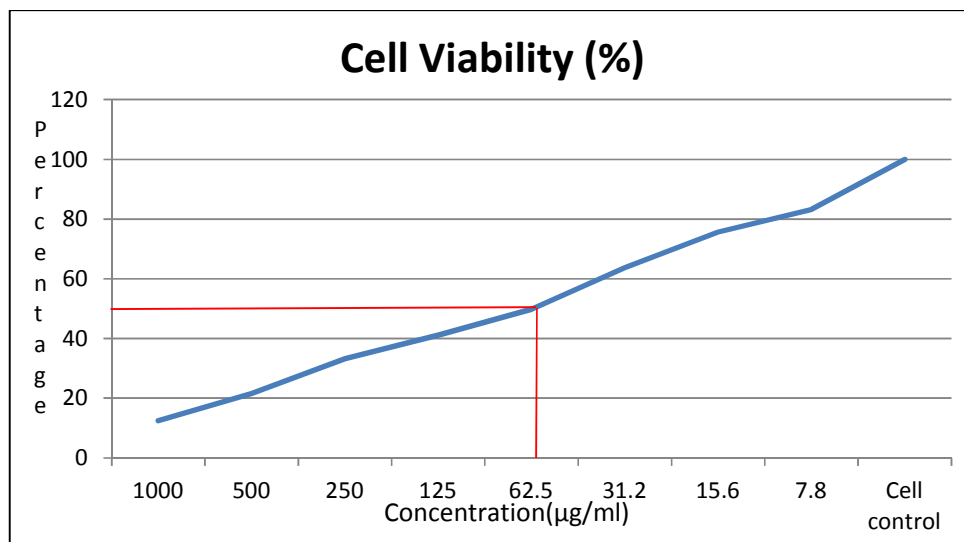


Fig. 10a.

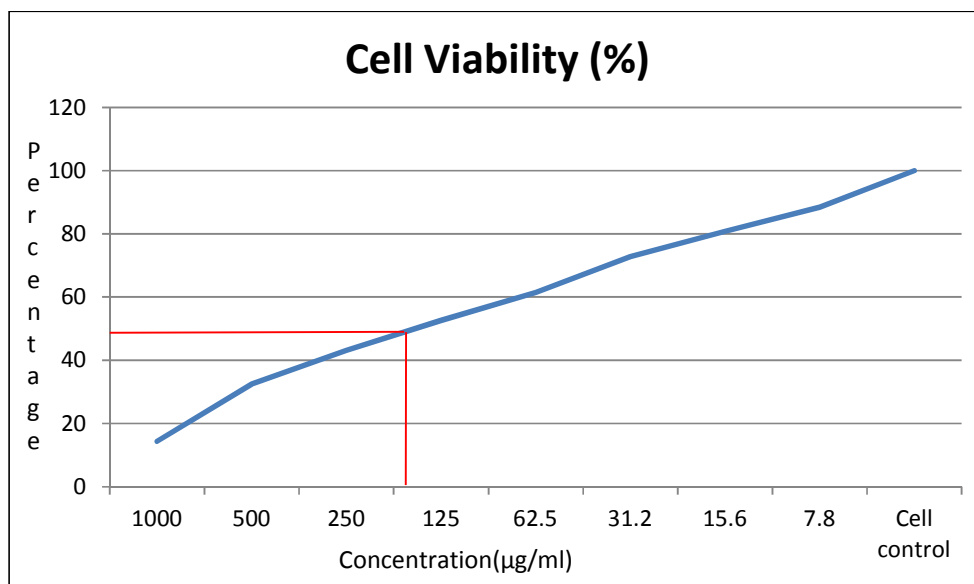


Fig. 10b.

Fig. 10 (a-b). Anticancer effect $\text{TiO}_2\text{-ZrO}_2$ and $\text{CeO}_2\text{-ZrO}_2$ on A549 cell line

4. CONCLUSION

Nanostructured CeO₂-ZrO₂ and TiO₂-ZrO₂ were successfully synthesized through ammonium Ce (IV) Nitrate and Titanium Isopropoxide by green combustion method. The advantages of the green preparation of NPs are simple and non-toxic. These NPs were confirmed by characterization of XRD. The result of SEM with EDX which reveals the physical structures and percentage of elements present in the composites. The synthesized NPs showed great activity against the bacterial pathogens as well as *In Vitro* cancer cell line. Our present study illustrated that these NPs can be considered further for *In vivo* studies.

CONSENT

It is not applicable.

ETHICAL APPROVAL

It is not applicable.

COMPETING INTERESTS

Authors have declared that no competing interests exist.

REFERENCES

- LunxiangY, WangY, PangG, KoltypinY, GedankenA. Sonochemical synthesis of cerium oxide nanoparticles effect of additives and quantum size effect, J. Coll. & Inter. Sci. 2002;246:78-84.
- ShahS, Md. ArifS, Reum Park A, Zhang K, Hyeok ParkJ, YooPJ. Green synthesis of biphasic TiO₂ reduced graphene oxide nanocomposites with highly enhanced photocatalytic activity, ACS Appl. Mater. & Inter. 2012;4:3893-3901.
- MarthaB, John Vohs M, Raymond Gorte J. Synthesis of highly porous yttria-stabilized zirconia by tape-casting methods. J. Am. Cer. Soc. 2003;86:395-400.
- RizwanN, MukhtarH, ManZ, MohshimDF. Material advancements in fabrication of mixed-matrix membranes, Chem. Eng. & Tech. 2013;36:717-727.
- Tsugio S, Shimada. Transformation of yttria-doped tetragonal ZrO₂ polycrystals by annealing in water. J. Am. Cer. Soc. 1985;68:356-356.
- ChangS, DoongR. Characterization of Zr-doped TiO₂ nanocrystals prepared by a nonhydrolytic sol-gel method at high temperatures, J. Phys. Chem. B. 2006; 110:20808-20814.
- Rakha EA, Putti TC, Abd El-Rehim DM, Paish C, Green AR, Powe DG, Lee AH, Robertson JF, Ellis IO. Morphological and immunophenotypic analysis of breast carcinomas with basal and myoepithelial differentiation. The Journal of Pathology. 2006;208:495-506.
- Wang Y, AnilkumarP, CaoL, Jia-Hui L, Pengju G, Kenneth N, Sahu S, WangP, WangX, SunYP. Carbon dots of different composition and surface functionalization: cytotoxicity issues relevant to fluorescence cell imaging, Exp. Bio. & Med. 2011;236:1231-1238.
- XiaoW, LiX, LiuD, SongS, ZhangH. Green synthesis of Pt/CeO₂/graphene hybrid nanomaterials with remarkably enhanced electrocatalytic properties, Chem. Commun. 2012;48:2885-2887.
- Deendayal M, Mark E, Bolander Mukhopadhyay D, Sarkar G, Mukherjee P. The use of microorganisms for the formation of metal nanoparticles and their application, Appl. Microbio. & Biotech. 2006;69:485-492.
- Tobias B, WickP, ManserP, Spohn P, GrassRN, LimbachLK, BruininkA, StarkWJ. *In vitro* cytotoxicity of oxide nanoparticles: comparison to asbestos, silica, and the effect of particle solubility, Env. Sci. & Tech. 2006;40:4374-4381.
- Nath RK, Nath SS, Sunar K. Sn-doped zinc oxide thin films for LPG sensors. J. Anal. Sci. Technol. 2012;3:85-94.
- Yu XY, Luo T, JiaY, Xu RX, Gao C, Zhang YX, Liu JH, Huang XJ. Three-dimensional hierarchical flower-like Mg-Al-layered double hydroxides: highly efficient adsorbents for As(V) and Cr(VI) removal, Nanoscale. 2012;4:3466-3474.
- Zhang GS, Liu HJ, Liu RP, Qu JH. Adsorption behavior and mechanism of arsenate at Fe-Mn binary oxide/water interface, J. Hazard. Mater. 2009;168:820-825.
- BozheyevF, Valiev D, NemkayevaR. Pulsed cathodoluminescence and Raman spectra of MoS₂ nanocrystals at different excitation electron energy densities and laser wavelengths, J. Lumine. 2017;188: 529-532.

16. Magdalane CM, Kaviyarasu K, Judith Vijaya J, Siddhardha B, Jeyaraj B. Photocatalytic activity of binary metal oxide nanocomposites of CeO₂/CdO nanospheres: Investigation of optical and antimicrobial activity. *J. Photochem. Photobiol. B Biol.* 2016;163:77-86.
17. Kaviyarasu K, Mariappan A, Neyvasagam K, Ayeshamariam A, Pandi P, Rajeshwara Palanichamy R, Gopinathan C, Genene T, Mola Maaza M. Photocatalytic performance and antimicrobial activities of HAp-TiO₂ nanocomposite thin films by sol-gel method. *Surfaces and Interfaces.* 2017;6:247-255.
18. Jesudoss SK, Judith Vijaya J, John Kennedy L, Iyyappa Rajan P, Hamad A, Al-Lohedan R, Jothi Ramalingam K, Kaviyarasu Bououdina M. Studies on the efficient dual performance of Mn_{1-x}Ni_xFe₂O₄ spinel nanoparticles in photodegradation and antibacterial activity. *J. Photochem. & Photobiol. B: Bio.* 2016;165:121-132.
19. Kaviyarasu K, Raja A, Devarajan PA. Structural elucidation and spectral characterizations of Co₃O₄ nanoflakes. *Spectrochimica Acta Part A: Molecular and Biomolecular Spectroscopy.* 2013;114:586-591.
20. Kaviyarasu K, Sajan D, Devarajan PA. A rapid and versatile method for solvothermal synthesis of Sb₂O₃ nanocrystals under mild conditions. *Applied Nanoscience.* 2013;3(6):529-533.
21. Chan CMN, Ng AMC, Fung MK, Cheng HS, Guo MY, Djuri AB, Fung FC, Chanc WK. Antibacterial and photocatalytic activities of TiO₂ nano-tubes. *J. Exp. Nanosci.* 2013;8:859-867.
22. Kaviyarasu K, Geetha N, Kanimozhi K, Maria Magdalane C, Sivaranjani S, Ayeshamariam A, Kennedy J, Maaza M. In vitro cytotoxicity effect and antibacterial performance of human lung epithelial cells A549 activity of zinc oxide doped TiO₂ nanocrystals: Investigation of biomedical application by chemical method. *Mater. Sci. & Eng.* 2017;74:325-333.
23. Angel Ezhilarasi A, Judith Vijaya J, Kaviyarasu K, Maaza M, Ayeshamariam A, John Kennedy L. Green synthesis of NiO nanoparticles using *Moringa oleifera* extract and their biomedical applications: Cytotoxicity effect of nanoparticles against HT-29 cancer cells. *J. Photochem. & Photobiol. B: Bio.* 2016;164:352-360.
24. K. Kaviyarasu, C.M. Magdalane, K. Anand, E. Manikandan, M. Maaza, Synthesis and characterization studies of MgO:CuO nanocrystals by wet-chemical method. *Spectrochimica Acta Part A: Molecular and Biomolecular Spectroscopy.* 2015;142: 405-409.
25. Kaviyarasu K, Devarajan PA. A convenient route to synthesize hexagonal pillar shaped ZnO nanoneedles via CTAB surfactant. *Adv. Mater.* 2013;4:582-585.
26. Magdalane CM, Kaviyarasu K, Vijaya JJ, Jayakumar C, Maaza M, Jeyaraj B. Photocatalytic degradation effect of malachite green and catalytic hydrogenation by UV-illuminated CeO₂/CdO multilayered nanoplatelet arrays: Investigation of antifungal and antimicrobial activities. *Journal of Photochemistry and Photobiology B: Biology.* 2017;169:110-123.
27. Kaviyarasu K, Kotsedi L, Aline Simo, Xolile Fuku Genene T, Mola Kennedy J, Maaza M. Photocatalytic activity of ZrO₂ doped lead dioxide nanocomposites: Investigation of structural and optical microscopy of RhB organic dye. *Applied Surface Science.* Available: <https://doi.org/10.1016/j.apsusc.2016.11.149>
28. Dumitriu C, Popescu M, Ungureanu C, Pirvu C. Antibacterial efficiencies of TiO₂ nanostructured layers prepared inorganic viscous electrolytes. *Appl. Sur. Sci.* 2015;341:157-165.
29. Kaviyarasu K, Kanimozhi K, Matinise N, Magdalane CM, Genene Mola T, Kennedy J, Maaza M. Antiproliferative effects on human lung cell lines A549 activity of cadmium selenide nanoparticles extracted from cytotoxic effects: Investigation of bio-electronic application. *Materials Science and Engineering. C* 2017;76: 1012-1025.
30. Sultana S, Mohammad Zain Khan R, Shahadat M. Development of ZnO and ZrO₂ nanoparticles: Their photocatalytic and bactericidal activity. *J. Env. Chem. Eng.* 2015;3:886-891.
31. Fuku X, Kaviyarasu K, Matinise N, Maaza M. Punicalagingreen functionalized Cu/Cu₂O/ZnO/CuO Nanocomposite for Potential Electrochemical Transducer and

- Catalyst. *Nanoscale Research*. 2016;11(1): 386.
32. Maria Magdalane C, Kaviyarasu K, Judith Vijaya J, Siddhardha B, Jeyaraj B. Facile synthesis of heterostructured cerium oxide/yttrium oxide nanocomposite in UV light induced photocatalytic degradation and catalytic reduction: Synergistic effect of antimicrobial studies, *Journal of Photochemistry and Photobiology B: Biology*. online 20 May 2017, In Press, Accepted Manuscript; 2017. Available: <https://doi.org/10.1016/j.jphotobiol.2017.05.024>
33. Magdalane CM, Kaviyarasu K, Judith Vijaya J, Jayakumar C, Maaza M, Jeyaraj B. Photocatalytic degradation effect of malachite green and catalytic hydrogenation by UV-illuminated CeO₂/CdO multilayered nanoplatelet arrays: Investigation of antifungal and antimicrobial activities, *J. Photochem. Photobiol. B: Bio*. 2017;169:110-123.
34. Frankfurt OS, Krishan A. Apoptosis-based drug screening and detection of selective toxicity to cancer cells. *Anticancer Drugs*. 2003;14:555-561.
35. Matinise N, Fuku XG, Kaviyarasu K, Mayedwa N, Maaza M. ZnO nanoparticles via *Moringa oleifera* green synthesis: Physical properties & mechanism of formation, *Applied Surface Science*. 2017;406:339-347.
36. Kaviyarasu K, Maria Magdalane C, Manikandan E, Jayachandran M, Ladchumananandasivam R, Neelamani S, Maaza M. Well-aligned graphene oxide nanosheets decorated with zinc oxide nanocrystals for high performance photocatalytic application, *International Journal of Nanoscience*. 2015;14(03):1550007.
37. Kaviyarasu K, Manikandan E, Nuru ZY, Maaza M. Investigation on the structural properties of CeO₂ nanofibers via CTAB surfactant, *Materials Letters*. 2015;160:61-63.
38. Kaviyarasu K, Murmu PP, Kennedy J, Thema FT, Douglas Letsholathebe L, Kotsedi M, Maaza M. Structural, optical and magnetic investigation of Gd implanted CeO₂ nanocrystals, *Nucl. Instr. Meth. B*; 2017. Available: <http://dx.doi.org/10.1016/j.nimb.2017.02.055>
39. Kasinathan K, Kennedy J, Manikandan E, Henini M, Maaza M. Photodegradation of organic pollutants RhB dye using UV simulated sunlight on ceria based TiO₂ nanomaterials for antibacterial applications, *Sci. Rep*. 2016;6:38064.

© 2019 Saleem et al.; This is an Open Access article distributed under the terms of the Creative Commons Attribution License (<http://creativecommons.org/licenses/by/4.0>), which permits unrestricted use, distribution, and reproduction in any medium, provided the original work is properly cited.

Peer-review history:

The peer review history for this paper can be accessed here:
<http://www.sdiarticle4.com/review-history/52799>